

CASE REPORT

Open Access



Imaging features of skeletal muscle lymphoma: a case report and literature review

Shuxi Gao¹, Hong Shu² and Hua Yang^{1*}

Abstract

Background: Diffuse large B cell lymphoma (DLBCL) is the most common type of non-Hodgkin lymphoma (NHL), occurring predominantly in older people. Skeletal muscle lymphoma is a rare form of DLBCL, most frequently affecting the thigh, upper extremities, calf, and pelvis.

Case presentation: We report a case of skeletal muscle DLBCL that was diagnosed using ultrasound (US)-guided biopsy. A 70-year-old man presented with progressive swelling and pain in the left lower extremity and an elevated erythrocyte sedimentation rate (ESR) and serum C-reactive protein (CRP), ferritin, and CA125 levels. US, magnetic resonance imaging (MRI), and computed tomography (CT) showed diffuse lesions in several muscles of the left lower extremity. Positron emission tomography/CT (PET/CT) showed FDG-uptake in the affected muscles. The patient was treated with chemotherapy and achieved a good response. A systematic review of the literature published between 1992 and 2019 was conducted to investigate the role of imaging, including imaging-guided biopsy, in the diagnosis of skeletal muscle lymphoma.

Conclusions: Skeletal muscle lymphoma is rare. US and MRI features include enlargement of muscular structures, with preservation of the architecture of the tissue and surrounding anatomical structures. Definitive diagnosis relies on histological and immunohistological analysis of a sample obtained through imaging-guided biopsy.

Keywords: Lymphoma, Skeletal muscle, Ultrasound, Biopsy, Imaging, Case report

Background

Lymphoma is a heterogeneous group of malignancies of lympho-reticular origin. Lymphomas can arise anywhere in the body and are traditionally divided into Hodgkin and non-Hodgkin lymphoma (NHL). Extranodal lymphoma involves sites other than lymph nodes, including the gastrointestinal tract, lung, central nervous system, salivary glands, thyroid, and gonads [1]. Extranodal lymphoma involving the musculoskeletal system, including bone, cutaneous/subcutaneous tissue and muscle, is rare [2]. The reported frequency of muscle lymphoma

accounts for 0.1% to 1.4% of all extranodal lymphomas and 1.2–2.0% of all malignant muscle tumors [3].

NHL is classified into B cell or T cell lymphomas. Diffuse large B cell lymphoma (DLBCL) is the most common type of NHL, occurring predominantly in older people [4]. Skeletal muscle lymphoma is a rare form of DLBCL, most frequently affecting the thigh, upper extremities, calf, and pelvis [2]. Patients with skeletal muscle lymphoma usually present with a progressively enlarging mass, swelling, pain, fever, sweating, and weight loss [5].

Imaging modalities, including computed tomography (CT), ultrasound (US) and magnetic resonance imaging (MRI), have been utilized to evaluate skeletal muscle lymphoma, and imaging characteristics of skeletal muscle lymphoma have been reported in small case series and case reports. However, diagnosis based on imaging

*Correspondence: yangh1@sj-hospital.org; yanghua2020cmu@163.com

¹ Department of Ultrasound, Shengjing Hospital of China Medical University, Shenyang 110004, Liaoning Province, Republic of China
Full list of author information is available at the end of the article



criteria alone is not conclusive, as imaging features of skeletal muscle lymphoma are variable.

Image-guided biopsies provide a safe and effective method for the conclusive diagnosis of musculoskeletal tumors [6]. US is frequently used as the initial imaging modality for evaluating a superficial symptomatic mass, and percutaneous US-guided biopsy is a convenient, radiation-free, and relatively inexpensive choice for biopsy of musculoskeletal soft tissue lesions [7]. Here, we report a case of skeletal muscle DLBCL of the lower extremity that was diagnosed by histological and immunohistological analysis of a sample obtained through percutaneous US-guided biopsy. We conducted a systematic review of the literature published between 1992 and 2019 to investigate the role of imaging, including imaging-guided biopsy, in the diagnosis of skeletal muscle lymphoma.

Case presentation

A 70-year-old Chinese male was admitted to the General Surgery Department of Shengjing Hospital (an affiliate of China Medical University) due to a 3 month history of fever and progressive swelling and pain in the left lower extremity in the absence of trauma or infection. The patient attended his local hospital when the symptoms began. There, a Color Doppler US examination showed dilated deep and intramuscular veins of the left lower extremity, with slow blood flow; therefore, intramuscular venous thrombosis of the calf was suspected. US examination revealed decreased echogenicity of the muscles of the medial and posterior compartments of the left thigh and the muscles of the posterior compartment of the calf, with a diffuse increase in vascularity. Blood tests showed an elevated D-dimer level, white blood cells were $8.04 \times 10^9/l$, monocytes were 11.90%, neutrophils were 76.30%, red blood cells were $3.61 \times 10^{12}/l$, and hemoglobin was 95 g/L. The diagnosis was suspected left calf intramuscular venous thrombosis, possibly due to cellulitis. The patient was given anticoagulation and parenteral antibiotics, including 800,000 units penicillin G sodium qd (i.v), 110 mg dabigatran ester bid (i.v), an antipyretic, and nutritional support. The swelling, pain and fever worsened, with a maximum temperature of 42 °C.

The patient was transferred to our institution. He had no relevant medical or family history, and he reported no history of weight loss or change in appetite. General physical examination was unremarkable. There were no signs of hepatosplenomegaly or abdominal, respiratory or cardiovascular disorders. On clinical examination, a hard, non tender, ill-defined mass was present in the left inguinal region. The left lower extremity was obviously swollen and tender, and the skin was dark red in color and warm to touch (Fig. 1). Neurological examination was normal.



Fig. 1 The left lower extremity was obviously swollen, and the skin was dark red in color

Routine blood and liver function tests were normal. Laboratory tests showed serum C-reactive protein (CRP) was 292.0 mg/L (normal 0–8), erythrocyte sedimentation rate (ESR) was 58 mm/h (normal 0–15), ferritin was 993.7 ng/ml (normal 11–336.2), CA125 was 66.32 U/mL (normal 0–35), β_2 -microglobulin (b2-MG) was 9.42 mg/L (normal 0.7–1.8), and lactic acid dehydrogenase (LDH) was normal. IgG and IgA levels were decreased.

US examination of the left lower extremity revealed large ill-defined hypoechoic regions within the muscles of the medial and posterior compartments of the thigh and the muscles of the posterior compartment of the calf, which were diffusely swollen, with preservation of the underlying muscle architecture. The regions were located at the margin or on one side of the muscles, irregularly infiltrating normal muscle tissue, with texture resembling muscle fibers retaining continuity with the surrounding muscles. Adjacent anatomical structures and tissues preserved their normal architecture. Color and power Doppler US showed hypervascularity within the regions (Fig. 2), but no evidence of thrombosis of the deep or superficial veins of the left lower limb. An enlarged lymph node was detected in the left inguinal area. On ultrasound, the inguinal lymph node had a thick hypoechoic periphery, a hyperechoic central region, and a clear distinction of the border of the cortex and medulla. Lymph node vascularity was increased and had a branch-like distribution. Increased echogenicity in the

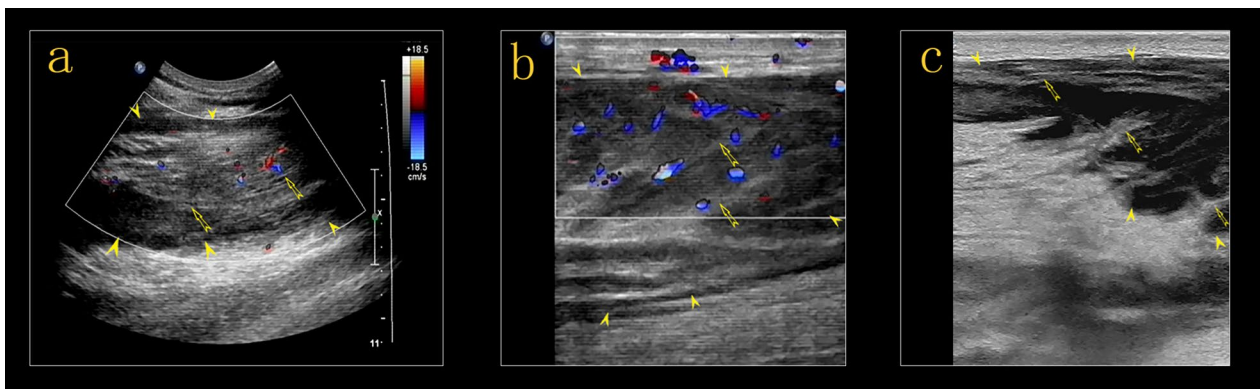


Fig. 2 Ultrasound examination of the left lower extremity revealed large poorly defined hypoechoic regions (*arrow head*) within the muscles of the medial compartment of the thigh (**a**) and gastrocnemius (**b, c**). The hypoechoic regions irregularly infiltrated normal muscle tissue, with texture resembling muscle fibers retaining continuity with the surrounding muscles (*arrow*). The architecture of the adjacent muscles appeared to be preserved. Color and power Doppler ultrasound showed hypervascularity (**a, b**)

subcutaneous tissues indicated edema. The provisional diagnosis was an intramuscular lesion.

Subsequently, MRI and CT were performed. Contrast-enhanced CT was used to evaluate the pelvic cavity and lower abdominal cavity, while MRI was used to evaluate the lower leg lesions. MRI of both calves showed diffuse swelling that infiltrated the muscles of the posterior compartment of the left calf. The distal aspect of the gastrocnemius and soleus had a minimally heterogeneous hypointense signal on T1-weighted images and a hyperintense signal on T2-weighted and fat suppression sequences (Fig. 3), with an ill-defined margin. Muscle fibers could be seen in some lesions, but they were indistinct. CT scans were performed on the lower abdomen and bilateral thighs. Non-contrast CT showed diffuse swelling of the muscles of the medial and posterior

compartments of the thigh. The muscles were enlarged, and contained patchy hypodense regions, with indistinct margins. Fat planes between muscles were lost. After intravenous contrast administration, enhancement of the involved muscles was slightly patchy, and mild. Attenuation after contrast administration did not appear to be substantially different from other muscle groups when compared to the contralateral side or the quadriceps muscle or gluteal bellies on the same side. The vessels enhanced as they normally would and probably appeared more conspicuous as compartmental compression impairs blood flow (Fig. 4). Abdominal and chest CT scans were normal.

The patient was provisionally diagnosed with intramuscular lesions; however, it is challenging to base a pathological diagnosis on imaging characteristics alone.



Fig. 3 Sagittal T1-weighted images (**a**), T2-weighted images with fat suppression (**b**), and axial T2-weighted images with fat suppression (**c**) showing diffuse swelling that infiltrated the gastrocnemius (*arrow head*), a minimally heterogeneous hypointense signal on T1-weighted images, a hyperintense signal on T2-weighted sequences (*arrow* in **a, b**), and an ill-defined boundary

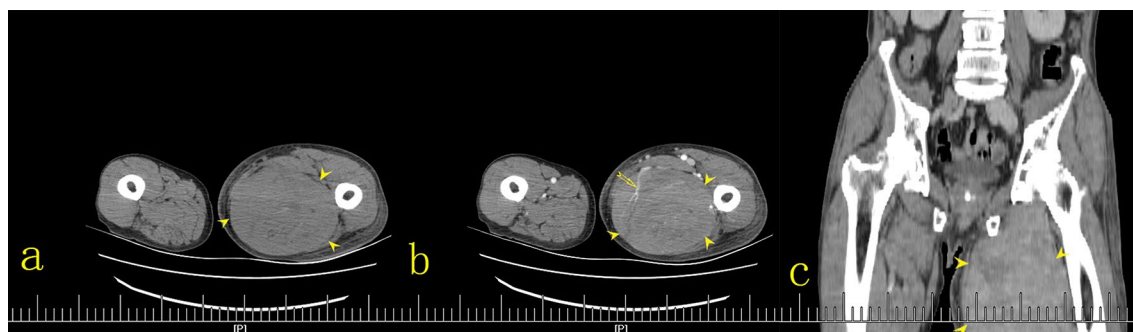


Fig. 4 Axial plain (a), intravenous-contrast-enhanced (b), and coronal reconstruction-contrast-enhanced (c) CT scans showing diffuse swelling of the muscles of the medial compartment and posterior compartment of the thigh. Muscles were enlarged and contained patchy hypodense regions, with indistinct margins (arrow head). The vessels enhanced as they normally would and probably appeared more conspicuous as compartmental compression impairs blood flow (arrow in b). Following intravenous contrast administration, there was slightly patchy and mild enhancement of the lesions (b, c)

Extensive patchy lesions and elevated inflammatory markers were consistent with inflammation, while a tumor that irregularly infiltrated the muscle suggested a different diagnosis, necessitating imaging-guided biopsy. Consequently, percutaneous US-guided core needle biopsy was performed under local anesthesia (2% lidocaine) using a 16 gauge needle. The hypoechoic solid-appearing parts of the regions within the gastrocnemius were targeted, while large blood vessels and nerves were avoided (Fig. 5). Four cores were obtained after four passes, without any immediate complications.

Biopsy specimens were fixed in 10% buffered formalin, processed, and embedded in paraffin. Microscopic examination revealed small round lymphoid cells arranged in

diffuse sheets. On immunohistochemistry, tumor cells were positive for CD20, CD19, vimentin, Bcl-2, Bcl-6 and MUM-1, scattered positive for CD5, cyclin D1 and P53 protein, and negative for CK, CD21, CD23, CD3, CD10 and desmin. The Ki-67 proliferation index was 90%. In situ hybridization was positive for Epstein-Barr encoded RNAs (EBER). The histopathological diagnosis was non-Hodgkin DLBCL (Fig. 6).

A staging whole body fluorodeoxyglucose (FDG)-positron emission tomography (PET) was performed to identify other sites of disease. F18-fluorodeoxyglucose PET/CT (F18-FDG PET/CT) demonstrated avid uptake in the left obturator externus muscle, the muscles of the medial and posterior compartments of the thigh, and the

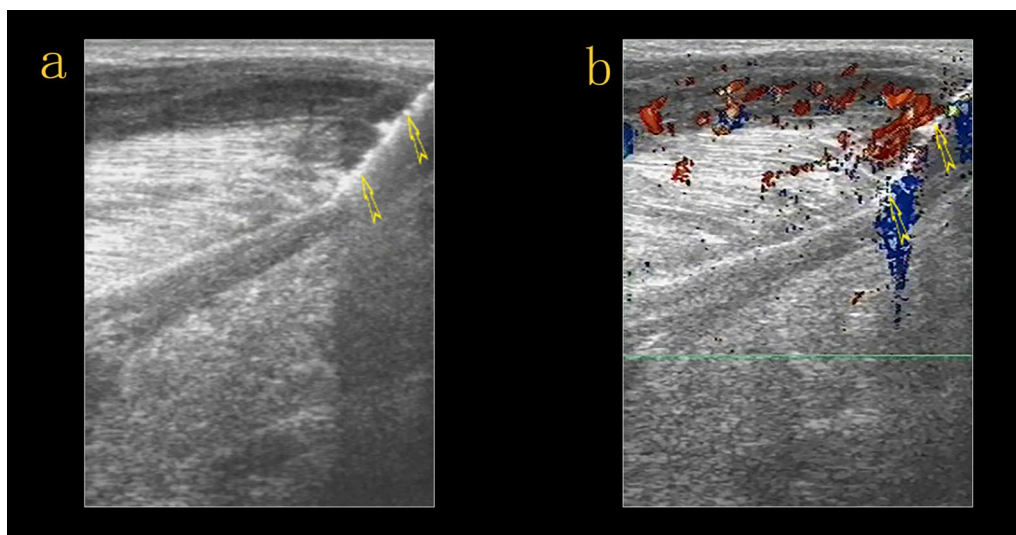


Fig. 5 Percutaneous US-guided biopsy of the hypoechoic solid-appearing parts of the lesions within the gastrocnemius (arrow)

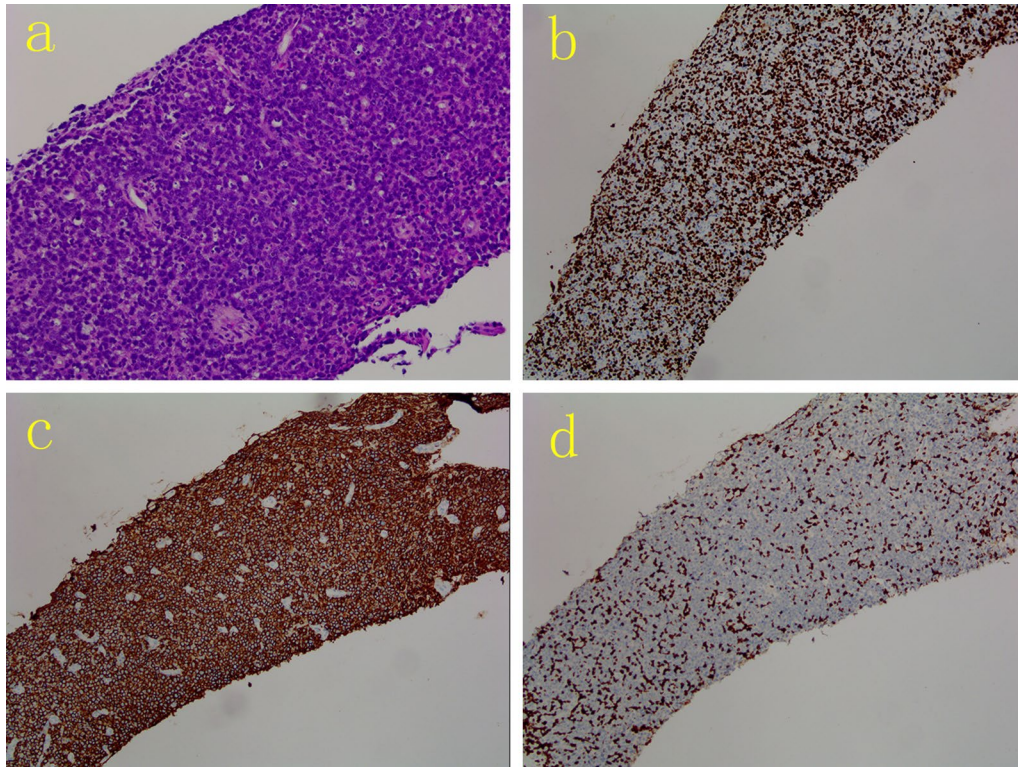


Fig. 6 Histopathological findings (**a**; hematoxylin–eosin [H&E] staining, 200 ×) showing medium sized tumor cells arranged in diffuse sheets, and immunohistochemical (IHC) staining (**b–d**; 100 ×) showing the Ki-67 proliferation index was 90% (**b**), and tumor cells were positive for CD20 (**c**) and negative for CD3 (**d**)

posterior and peroneal muscles of the calf (maximum standard uptake value [SUV_{max}] = 10.2) (Fig. 7). Enlarged lymph nodes with increased FDG-uptake were observed in the left inguinal region. Bone marrow biopsy was normal, showing no evidence of lymphoma.

The patient was referred to the Haematology Department for chemotherapy where he was started on rituximab, cyclophosphamide, doxorubicin, vincristine, and prednisone (R-CHOP). To date, the patient has received four cycles (21 days each) of R-CHOP according to the

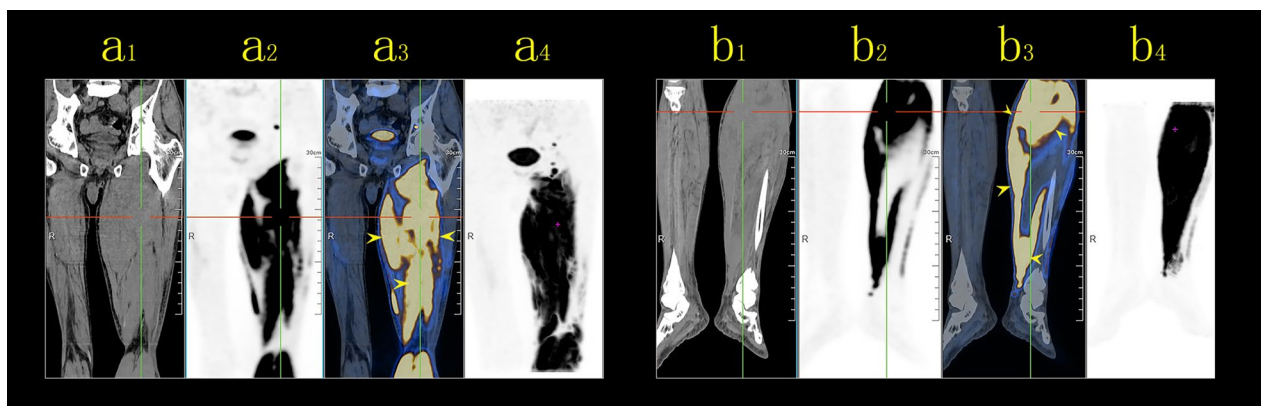


Fig. 7 Positron emission tomography/computed tomography (PET/CT) showing multiple lesions of increased FDG-uptake in the left obturator externus muscle, the muscles of the medial and posterior compartments of the thigh (**a**), and the posterior and peroneal muscles of the calf (**b**). (a1 & b1) CT image showing ill-defined intramuscular lesions. (a3 & b3) PET/CT image showing multiple lesions with FDG uptake (maximum standardized uptake: 10.20). (a2, a4 and b2, b4) FDG images



Fig. 8 The swelling in the left lower extremity was completely resolved, but the skin remained pigmented

following protocol: Day 1, 600 mg rituximab qd (quaque die) (intravenous pump); Days 2–4, 700 mg cyclophosphamide qd (intravenous drip); Day 2, 20 ml doxorubicin qd (intravenous drip); Day 2, 5 mg vincristine qd (intravenous drip); Days 2–6: 15 mg dexamethasone qd (intravenous drip). The patient achieved a satisfactory initial response, and the swelling of the left lower extremity gradually subsided. After the fourth cycle of R-CHOP, the swelling in the left lower extremity was completely resolved, but the skin remained pigmented (Fig. 8). US revealed obvious regression of the hypoechoic regions in the muscles of the medial and posterior compartments of the left thigh and the gastrocnemius, and on Color Doppler US, vascularity was decreased compared to the initial examination (Fig. 9). At the end of treatment, the patient underwent another US examination, which showed the size of the hypoechoic regions had decreased and the vascularity of the affected muscles was substantially reduced and only slightly greater than normal peripheral muscles. The patient is receiving regular follow-up. Eighteen months after the initial presentation in August 2019, the patient was considered clinically well and showed no signs or symptoms of lymphoma.

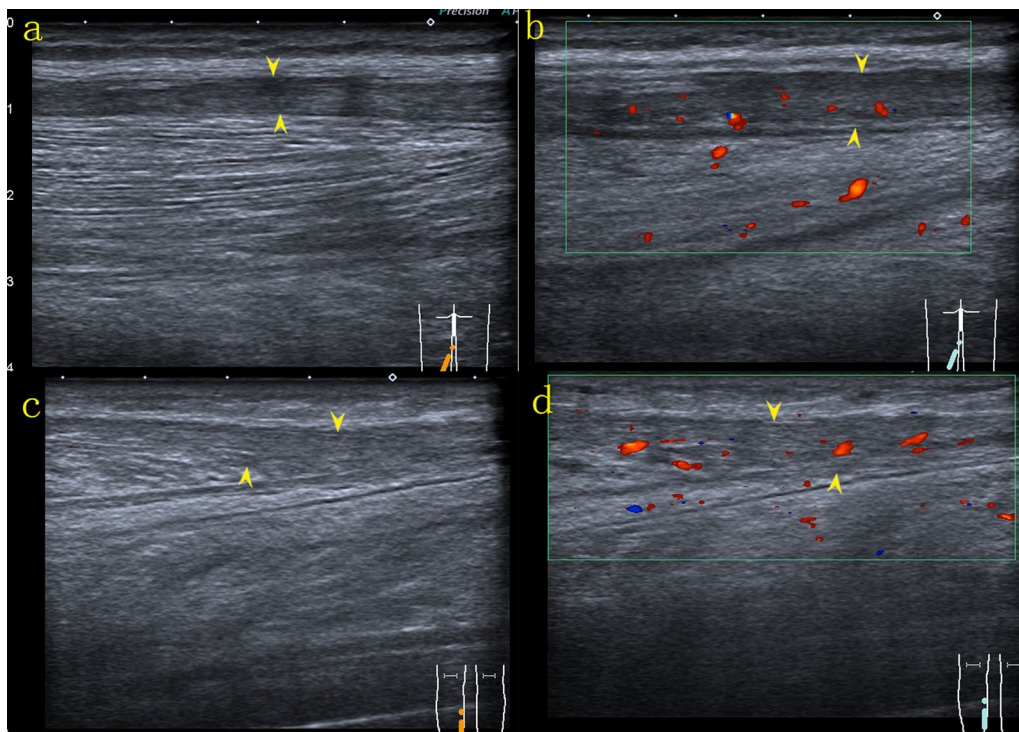


Fig. 9 Ultrasound revealed obvious regression of the lesions, and the adductor muscles of the left thigh (a, b) and the gastrocnemius (c, d) were clearly defined with decreased peripheral echogenicity (arrow head). On color Doppler ultrasound, the vascularity of the affected muscles was decreased compared to the initial examination (b, d)

Discussion and conclusions

In this report, we present a rare case of skeletal muscle DLBCL occurring in the lower extremity of a patient who had not experienced trauma or infection but who was positive for EBV. Evidence suggests that the majority of skeletal muscle lymphomas are non-Hodgkin B-cell tumours [8], with DLBCL as the most common extranodal manifestation of lymphoma involving skeletal muscle. The diagnosis of DLBCL requires multiple tests, including immunohistochemical studies, fluorescent in situ hybridization, polymerase chain reaction techniques, and occasionally, next generation sequencing [9]. Immunohistochemical staining for MYC, Bcl-2 and Bcl-6 may predict and guide treatment options in DLBCL [9]. Skeletal muscle DLBCL is frequently located in the lower extremities, especially the thigh [10–12], and usually occurs after leg injury or needle injections [12, 13]. EBV is a risk factor associated with a variety of tumours, including B and T-cell lymphomas and smooth muscle tumors [13]. Based on immunophenotype, our case is best classified as an EBV-positive DLBCL.

Skeletal muscle lymphoma is rare, with only a few cases described in the published literature. Skeletal muscle lymphoma may be primary extranodal or secondary to invasion from adjacent bone or lymph nodes, metastasis from disseminated disease, or primary extra-nodal muscle lymphoma [14, 15]. Skeletal muscle lymphoma usually presents as a painful unilateral limb swelling, representing a diagnostic challenge when differentiating muscle lymphoma from deep vein thrombosis or soft tissue tumors such as sarcoma, rhabdomyosarcoma, rhabdomyoblastoma, melanoma, and osteosarcoma [16]. Accurate diagnosis of skeletal muscle lymphoma is necessary to avoid unnecessary excisions when other entities are suspected.

Imaging tools play a critical role in the diagnosis of skeletal muscle lymphoma. On radiologic examination, skeletal muscle lymphoma appear as focal intramuscular masses and diffuse muscle enlargement with tumor infiltration [3]. Muscle enlargement is the most common pattern [3]; however, there are no specific radiologic criteria for diagnosing skeletal muscle lymphoma.

To further investigate the role of imaging in the definitive diagnosis of skeletal muscle lymphoma, a systematic review of the literature published between 1992 and 2019 was conducted. The PubMed database was searched using the Mesh terms: “lymphoma”, “muscular”, “skeletal”, “soft tissue”, and “image.” Relevant case reports and case series, reviews, and retrospective studies describing skeletal muscle lymphoma were retrieved. Studies reporting on patients with a history of lymphoma at another site, skeletal muscle lymphoma arising from adjacent tumors, other systemic disease such as HIV

infection, rhabdomyolysis or sarcoidosis or other organ involvement, studies with no detailed description of the radiologic features of skeletal muscle lymphoma, or literature reviews, were excluded. Searches were restricted to the English language. Finally, 25 full-text articles were reviewed, and the imaging features of 95 patients with skeletal muscle lymphoma on US, MRI (non- or contrast), CT (non- or contrast) and PET/CT, including those described for the present case, are summarized in Table 1 and Fig. 10. Findings showed the imaging features of skeletal muscle lymphoma included enlargement of muscular structures, with preservation of the architecture of the tissue and surrounding anatomical structures. Most cases were finally diagnosed by imaging-guided biopsy. To our knowledge, this is the most extensive review of the imaging features of skeletal muscle lymphoma currently available in the published literature.

MRI has been considered the most useful modality for assessment of skeletal muscle lymphoma [17]; however, MRI is costly, patients may have contraindications, and MRI characteristics of skeletal muscle lymphoma are nonspecific and sometimes contradictory. Studies have reported skeletal muscle lymphoma appear hypointense, isointense, or slightly hyperintense relative to surrounding muscle on T1-weighted images and mostly hyperintense on T2-weighted and fat suppression sequences [5, 18–21]. Contrast-enhanced MRI has shown diffuse homogeneous or heterogeneous enhancement [5, 11], peripheral thick band-like enhancement, marginal septal enhancement, or deep fascial enhancement [17, 22], which may have been caused by multicompartiment infiltration [22]. One report [23] described a case of skeletal muscle lymphoma with no contrast enhancement in any of the affected muscles. Several features on MRI are suggestive of skeletal muscle lymphoma and may serve to differentiate skeletal muscle lymphoma from other intramuscular malignant tumours. These include infiltration of the subcutaneous fat with occasional skin thickening or edema [5, 11, 15, 22], although this was not observed in the present case; multicompartiment muscle involvement [5, 15, 24]; tumor extension along neurovascular bundles or muscle fascicles; and vessels traversing the affected muscles [15, 17].

US is helpful for delineating soft tissue lesions. On US, skeletal muscle lymphoma may be suspected in cases showing diffuse muscle enlargement with multicompartiment muscle involvement and swelling of muscle bundles. Skeletal muscle lymphoma may appear as homogeneous or heterogeneous hypoechoic masses with lobulated, irregular, well or poorly defined margins and coarsened fibroadipose septa [3, 8, 11, 17, 25, 26], or hypoechoic regions with texture resembling muscle fibers retaining continuity with the surrounding muscles,

Table 1 Published studies describing the imaging features of extranodal lymphoma of muscle (listed chronologically)

Literature Author/ year	General information			US			MRI			CT			PET/CT (N)	
	(Sex, N)/ age	Number of affected muscles (N)	Boundary (N)	Echogenicity (N)	Vascularity (N)	Boundary (N)	T1W (N)	T1W + Gd (N)	T2W (N)	STIR (N)	Boundary (N)	Plain (N)		Contrast (N)
Metzler et al. [23]	F/65	Multiple	-	-	-	N/A	Hypoin- tense	No enhance- ment	Hypoin- tense	Hyperin- tense	-	-	-	-
Eustace et al. [34]	(F, 2)/ (67,68)	Single	-	-	-	Well- defined (1), N/A (1)	Isointense	Diffuse enhance- ment (1), N/A (1)	Hyperin- tense	Hyperin- tense (1), N/A (1)	-	-	-	-
Panicek et al. [30]	(M, 2)/ (68,77)	Multiple (1), single (1)	-	-	-	N/A	N/A	N/A	N/A	N/A	N/A	Isodense to hypodense	Moderate enhance- ment	-
Beggs [11]	(M, 4; F, 2)/ (31–76)	Multiple (5), single (1)	Ill-(3), well-(2) defined, N/A (1)	Hypochoic (4), fibroadi- pose septa and swollen muscle bundles (1), patchy distal acoustic enhancement (1), N/A (1)	N/A	Ill-(3), well- (2) defined, N/A (1)	Minimally hyperin- tense (3), isointense (1), N/A (2)	Heteroge- neous (1), diffuse (1), patchy (1) enhance- ment, N/A (3)	Hyperin- tense (4), N/A (2)	Hyperin- tense (2), N/A (4)	Ill-(1), well- (1) defined, N/A (4)	Isodense	Isodense (1), N/A (5)	-
Lee et al. [5]	(M, 2; F, 3)/ (15–80)	Multiple (2), single (3)	-	-	-	N/A	Isointense	N/A	Hyperin- tense	N/A	N/A	Isodense to hypodense (2), N/A (3)	N/A	Increased uptake (2), N/A (3)
Suresh et al. [15]	(M, 14; F, 10)/ (15–80)	Multiple (12), single (12)	-	-	-	Ill- (16) or well- (8) defined	Hyperin- tense (15), isointense (8), N/A (1)	Homoge- neous or hetero- geneous enhance- ment	Hyperin- tense (1), isointense (21), N/A (2)	Hyperin- tense (16), N/A (8)	-	-	-	-
Laffosse et al. [14]	F/66	Single	N/A	Hypochoic	N/A	N/A	Isointense	Enhance- ment	N/A	N/A	-	-	-	-
Wu et al. [35]	M/14	Multiple	N/A	Hypochoic	N/A	N/A	N/A	Enhance- ment	Markedly hyperin- tense	N/A	Ill-defined	N/A	N/A	-
Driss et al. [20]	M/8	Multiple	-	-	-	N/A	Hypoin- tense	N/A	Hyperin- tense	N/A	N/A	N/A	N/A	-

Table 1 (continued)

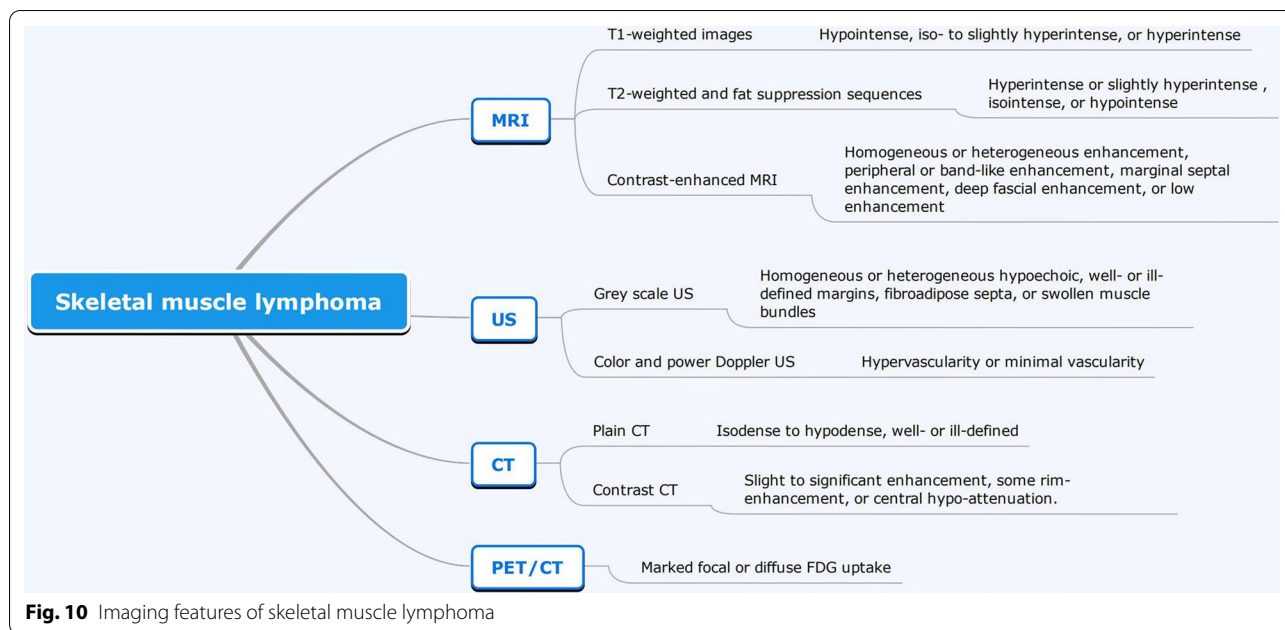
Literature Author/year	General information			US			MRI			CT			PET/CT (N)
	(Sex, N)/age	Number of affected muscles (N)	Boundary (N)	Echogenicity (N)	Vascularity (N)	Boundary (N)	T1W (N)	T1W + Gd (N)	T2W (N)	STIR (N)	Boundary Plain (N)	Contrast (N)	
Broski et al. [36]	M/65	Multiple	-	-	-	N/A	N/A	N/A	N/A	N/A	-	-	Increased uptake
Chun et al. [22]	(M, 14; F, 6)/(5-90)	Multiple (14), single (6)	-	-	-	N/A	Intermediate (11), hyperintense (9)	Diffuse (13), peripheral band (4), marginal septal (2), enhancement, N/A (1)	Isointense	Hyperintense (5), isointense (8), N/A (7)	-	-	-
Gaiser et al. [37]	M/10	Single	-	-	-	Ill-defined	N/A	Vivid enhancement	N/A	N/A	-	-	-
Muralee Mohan et al. [26]	M/55	Single	Ill-defined	Hypochoic, muscle like texture	Minimal	N/A	Isointense	N/A	Heterogeneously hyperintense	Hyperintense	Well defined	Homogeneous enhancement	-
Carroll et al. [18]	(M, 2; F, 5)/(56-68)	Multiple (2), single (5)	-	-	-	Ill-(3) or well-(4) defined	Iso to slightly hyperintense	Homogeneous enhancement	Homogeneously or heterogeneously hyperintense	N/A	-	-	-
Hongsakul et al. [38]	F/45	Multiple	Ill-defined	Hypochoic, fibroadipose septa and swollen muscle bundles	N/A	N/A	Slightly hyperintense	Inhomogeneous enhancement	Slightly hyperintense	N/A	N/A	Enlargement	Enhancement
Surov [3]	(M, 4; F, 6)/(45-75)	Multiple (1), single (9)	-	-	-	N/A	Homogeneously hypointense	N/A	Hyperintense	Hyperintense	-	-	-

Table 1 (continued)

Literature	General information			US			MRI			CT			PET/CT (N)		
	Author/ year	(Sex, N)/ age	Number of affected muscles (N)	Boundary (N)	Echogenicity (N)	Vascularity (N)	Boundary (N)	T1W (N)	T1W + Gd (N)	T2W (N)	STIR (N)	Boundary Plain (N)		Contrast (N)	
Katsura et al. [33]	F/52		Multiple	-	-	-	-	-	-	-	-	N/A	Non-uniformly early enhancing, central necrosis	Increased uptake	
Zhang et al. [39]	F/76		Multiple	N/A	Hypoechoic	N/A	N/A	N/A	Enhancement	N/A	N/A	-	-	-	
Hatem et al. [32]	M/70		Single	Ill-defined	Hypoechoic	N/A	Ill-defined	N/A	N/A	N/A	N/A	-	-	Increased uptake	
Elkourashy et al. [40]	M/40		Multiple	-	-	-	N/A	Abnormal	Heterogeneous enhancement	N/A	N/A	-	-	-	
Burton et al. [41]	M/17		Multiple	-	-	-	N/A	Isointense	Diffuse enhancement	Diffusely mildly hyperintense	N/A	-	-	-	
Spetsieris et al. [29]	F/70		Multiple	N/A	Hypoechoic	Increased	N/A	Hypointense	Enhancement	Hyperintense	N/A	N/A	Isodense	N/A	
Martins et al. [42]	M/76		Multiple	-	-	-	Well-defined	Isointense	Peripheral enhancement	Hyperintense	Hyperintense	-	-	Increased uptake	
Binici et al. [43]	F/41		Multiple	-	-	-	Ill-defined	Isointense	N/A	Hyperintense	N/A	-	-	-	
Present case/2019	M/70		Multiple	Ill-defined	Hypoechoic, muscle fibers	Increased	Ill-defined	Minimally hyperintense	N/A	Hyperintense	N/A	Ill-defined	Hypodense	mild-moderate enhancement	Increased uptake

T1W T1-weighted sequence; T2W T2-weighted sequence; Gd gadolinium; STIR short-tau inversion recovery; US ultrasound; MRI magnetic resonance imaging; CT computed tomography; PET/CT positron emission tomography/computed tomography; N/A not available

N refers to the number of patients



as in the present case and one other previous study [26]. This feature has not been described in other intramuscular lesions such as sarcoma, myositis and inflammatory pseudotumors, and may be an important consideration for differential diagnosis. This feature may reflect the degree of muscle involvement [11, 27] and correlate with histological findings that show neoplastic lymphocytes surrounding and invading myofibrils [27, 28]. Color and power Doppler US may show hypervascularity [25, 29]. Real-time US-guided core needle biopsy is often used for diagnosis of skeletal muscle lymphoma, and was applied in the present case.

CT is frequently performed for initial evaluation of soft-tissue masses in patients for whom MRI may be contraindicated due to the presence of intracranial aneurysm clips, a cardiac pacemaker, or a predisposition to claustrophobia [25, 30]. CT characteristics of skeletal muscle lymphoma are nonspecific. On plain CT, skeletal muscle lymphoma may appear as swelling of the affected muscles with well- or ill-defined lesions that are homogeneous, isodense, hyperdense or hypodense to normal muscle [3, 5, 11, 25, 31]. On contrast CT, skeletal muscle lymphoma may show slight to significant enhancement [5, 11], some rim-enhancement, or central hypo-attenuation [31]. Other common malignancies of soft tissue, including malignant fibrous histiocytoma, fibrosarcoma and liposarcoma, also appear as heterogeneous masses with variable enhancement on CT [30] and must be differentiated from skeletal muscle lymphoma. Skeletal muscle lymphoma may be suspected where CT shows a homogeneous mass with attenuation similar to that of normal

muscle and traversing vessels in the affected muscle [30], as in the present case.

PET/CT fusion is an important imaging tool for initial staging, assessment of treatment efficacy, and restaging after treatment in patients with cancer [31]. In skeletal muscle lymphoma, there is usually marked focal or diffuse FDG uptake in the affected muscles, and uptake levels may be correlated with malignant potential; however, it is difficult to differentiate primary or secondary skeletal muscle lymphoma from other malignant tumours and inflammatory lesions. In the present case, PET/CT imaging showed increased FDG uptake in multiple muscles of the left thigh and calf.

The workup of patients with skeletal muscle lymphoma should include imaging, image-guided biopsy, histological examination of the biopsy to confirm the diagnosis, and clinical staging to select appropriate treatment. The combination of chemotherapy and immunotherapy (R-CHOP) with or without radiation therapy is considered standard therapy for DLBCL [32]. This approach achieves a good response in patients with skeletal muscle lymphoma [29, 32, 33]. However, a meta analysis [24] revealed that DLBCL of the soft tissue is aggressive and associated with poor prognosis, requiring further studies to better characterize this peculiar entity.

In conclusion, lymphoma arising in the skeletal muscle is rare. The majority of skeletal muscle lymphomas are B cell lymphomas, especially DLBCL. US, CT, and MRI can be used to identify muscle lymphoma. On US, skeletal muscle lymphoma should be suspected in patients presenting with lesions that appear as hypoechoic masses

containing residual muscle fibers or swollen muscle bundles and that involve multiple muscles. The definitive diagnosis of skeletal muscle lymphoma relies on histological and immunohistological analysis of a sample obtained through imaging-guided biopsy and proper staging, which inform clinical decision making.

Abbreviations

US: Ultrasound; CT: Computed tomography; MRI: Magnetic resonance imaging; CA125: Cancer antigen 125; IHC: Immunohistochemical; ESR: Erythrocyte sedimentation rate determination; CRP: C-reactive protein; B2-MG: B2 microglobulin; LDH: Lactate dehydrogenase.

Acknowledgements

None.

Authors' contributions

SXG wrote and revised the manuscript. HS performed the pathological imaging. HY edited the manuscript and imaging. All authors approved the final manuscript.

Funding

This study was supported by a research program of the National Natural Science Foundation of China (NSFC) under Grant No. 82001846.

Availability of data and materials

The datasets generated and analyzed during the present study are available from the corresponding author on reasonable request.

Declarations

Ethics approval and consent to participate

This study was approved by the ethics committee of Shengjing Hospital of China Medical University. All procedures were performed in accordance with the ethical standards of the institutional and/or national research committee and with the 1964 Helsinki declaration and its later amendments or comparable ethical standards. Written informed consent was obtained from the patient.

Consent to publish

Written informed consent for publication of this case report was obtained from the patient.

Competing interests

The authors declare that they have no conflict of interest.

Author details

¹Department of Ultrasound, Shengjing Hospital of China Medical University, Shenyang 110004, Liaoning Province, Republic of China. ²Department of Pathology, Shengjing Hospital of China Medical University, Shenyang, Liaoning Province, Republic of China.

Received: 15 December 2020 Accepted: 8 September 2021

Published online: 26 September 2021

References

- Freeman C, Berg JW, Cutler SJ. Occurrence and prognosis of extranodal lymphomas. *Cancer*. 1972;29:252–60.
- Murphey MD, Kransdorf MJ. Primary musculoskeletal lymphoma. *Radiol Clin N Am*. 2016;54:785–95.
- Surov A. Imaging findings of skeletal muscle lymphoma. *Clin Imaging*. 2014;38:594–8.
- Flowers CR, Sinha R, Vose JM. Improving outcomes for patients with diffuse large B-cell lymphoma. *CA Cancer J Clin*. 2010;60:393–408.
- Lee VS, Martinez S, Coleman RE. Primary muscle lymphoma: clinical and imaging findings. *Radiology*. 1997;203:237–44.
- Chang CY, Huang AJ, Bredella MA, Torriani M, Halpern EF, Rosenthal DI, et al. Percutaneous CT-guided needle biopsies of musculoskeletal tumors: a 5-year analysis of non-diagnostic biopsies. *Skelet Radiol*. 2015;44:1795–803.
- Loudini N, Glaudemans A, Jutte PC, Suurmeijer AJH, Yakar D, Kwee TC. The diagnostic significance of repeat ultrasound-guided biopsy of musculoskeletal soft-tissue lesions with initially inconclusive biopsy results. *Eur J Surg Oncol*. 2019;45:1266–73.
- Hill S, Dunn A, Thomas JM. Lymphoma presenting as an intramuscular mass. *Br J Surg*. 1997;84:1741–3.
- Beham-Schmid C. Aggressive lymphoma 2016: revision of the WHO classification. *Memo*. 2017;10:248–54.
- Samuel LM, White J, Lessells AM, Roddie H, Matheson LM. Primary non-Hodgkins lymphoma of muscle. *Clin Oncol (R Coll Radiol)*. 1999;11:49–51.
- Beggs I. Primary muscle lymphoma. *Clin Radiol*. 1997;52:203–12.
- Keung YK, Liang R. Report of a case of primary skeletal muscle lymphoma and review of the literature. *Acta Haematol*. 1996;96:184–6.
- Chevalier X, Amoura Z, Viard JP, Souissi B, Sobel A, Gherardi R. Skeletal muscle lymphoma in patients with the acquired immunodeficiency syndrome: a diagnostic challenge. *Arthritis Rheum*. 1993;36:426–7.
- Laffosse JM, Gomez-Brouchet A, Molinier F, Chiron P, Roche H, Puget J. A case of malignant primary non-Hodgkin's lymphoma in skeletal muscle treated by exclusive chemotherapy. *Jt Bone Spine*. 2009;76:86–8.
- Suresh S, Saifuddin A, O'Donnell P. Lymphoma presenting as a musculoskeletal soft tissue mass: MRI findings in 24 cases. *Eur Radiol*. 2008;18:2628–34.
- Alamdari A, Naderi N, Peiman S, Shahi F. Non-Hodgkin lymphoma with primary involvement of skeletal muscle. *Int J Hematol Oncol Stem Cell Res*. 2014;8:55–7.
- Lim CY, Ong KO. Imaging of musculoskeletal lymphoma. *Cancer Imaging*. 2013;13:448–57.
- Carroll G, Breidahl W, Robbins P. Musculoskeletal lymphoma: MRI of bone or soft tissue presentations. *J Med Imaging Radiat Oncol*. 2013;57:663–73.
- Ruzek KA, Wenger DE. The multiple faces of lymphoma of the musculoskeletal system. *Skelet Radiol*. 2004;33:1–8.
- Driss M, Abbas I, Mrad K, Sassi S, Oubich F, Barsaoui S, et al. Primary CD30/ALK-1 positive anaplastic large cell lymphoma of the skeletal muscle in a child. *Pathologica*. 2009;101:97–100.
- Surov A, Behrmann C. Diffusion-weighted imaging of skeletal muscle lymphoma. *Skelet Radiol*. 2014;43:899–903.
- Chun CW, Jee WH, Park HJ, Kim YJ, Park JM, Lee SH, et al. MRI features of skeletal muscle lymphoma. *AJR Am J Roentgenol*. 2010;195:1355–60.
- Metzler JP, Fleckenstein JL, Vuitch F, Frenkel EP. Skeletal muscle lymphoma: MRI evaluation. *Magn Reson Imaging*. 1992;10:491–4.
- Derenzini E, Casadei B, Pellegrini C, Argnani L, Pileri S, Zinzani PL. Non-hodgkin lymphomas presenting as soft tissue masses: a single center experience and meta-analysis of the published series. *Clin Lymphoma Myeloma Leuk*. 2013;13:258–65.
- Hwang S. Imaging of lymphoma of the musculoskeletal system. *Radiol Clin N Am*. 2008;46(379–96):x.
- Muralee Mohan C, Thakral A, Bhat SK. Primary extranodal non-Hodgkin's lymphoma involving masseter and buccinator muscles. *Int J Oral Maxillofac Surg*. 2012;41:1393–6.
- Masaoka S, Fu T. Malignant lymphoma in skeletal muscle with rhabdomyolysis: a report of two cases. *J Orthop Sci*. 2002;7:688–93.
- Dai Y, Sowjanya M, You J, Xu K. Non-Hodgkin's Lymphoma of Multiple Skeletal Muscles Involvement Seen on FDG PET/CT Scans. *Medicine (Baltimore)*. 2015;94:e833.
- Spetsieris N, Giannakopoulou N, Variami E, Zervakis K, Rougala N, Garafalakis G, et al. Isolated skeletal muscle recurrence of an originally nodal diffuse large B cell lymphoma: a case report and review of the literature. *Medicine (Baltimore)*. 2018;97:e9608.
- Panicek DM, Lautin JL, Schwartz LH, Castellino RA. Non-Hodgkin lymphoma in skeletal muscle manifesting as homogeneous masses with CT attenuation similar to muscle. *Skelet Radiol*. 1997;26:633–5.
- Surov A, Holzhausen HJ, Arnold D, Schmidt J, Spielmann RP, Behrmann C. Intramuscular manifestation of non-Hodgkin lymphoma and myeloma: prevalence, clinical signs, and computed tomography features. *Acta Radiol*. 2010;51:47–51.

32. Hatem J, Bogusz AM. An unusual case of extranodal diffuse large B-cell lymphoma infiltrating skeletal muscle: a case report and review of the literature. *Case Rep Pathol.* 2016;2016:9104839.
33. Katsura M, Nishina H, Shigemori Y, Nakanishi T. Extranodal lymphoma originating in the gluteal muscle with adjacent bone involvement and mimicking a soft tissue sarcoma. *Int J Surg Case Rep.* 2015;7C:161–4.
34. Eustace S, Winalski CS, McGowen A, Lan H, Dorfman D. Skeletal muscle lymphoma: observations at MR imaging. *Skelet Radiol.* 1996;25:425–30.
35. Wu L, Wang Y, Fu SL, Huang L, Tongji FC, Qi JY. Anaplastic large cell lymphoma with primary involvement of skeletal muscle: a rare case report and review of the literature. *Pediatr Hematol Oncol.* 2009;26:142–9.
36. Broski SM, Bou-Assaly W, Gross MD, Fig LM. Diffuse skeletal muscle F-18 fluorodeoxyglucose uptake in advanced primary muscle non-Hodgkin's lymphoma. *Clin Nucl Med.* 2009;34:251–3.
37. Gaiser T, Geissinger E, Schattenberg T, Scharf HP, Durken M, Dinter D, et al. Case report: a unique pediatric case of a primary CD8 expressing ALK-1 positive anaplastic large cell lymphoma of skeletal muscle. *Diagn Pathol.* 2012;7:38.
38. Hongsakul K, Laohawiriyakamol T, Kayasut K. A rare case of primary muscular non-Hodgkin's lymphoma and a review of how imaging can assist in its diagnosis. *Singap Med J.* 2013;54:e179–82.
39. Zhang L, Lin Q, Zhang L, Dong L, Li Y. Primary skeletal muscle diffuse large B cell lymphoma: a case report and review of the literature. *Oncol Lett.* 2015;10:2156–60.
40. Elkourashy SA, Nashwan AJ, Alam SI, Ammar AA, El Sayed AM, Omri HE, et al. Aggressive lymphoma "sarcoma mimicker" originating in the gluteus and adductor muscles: a case report and literature review. *Clin Med Insights Case Rep.* 2016;9:47–53.
41. Burton E, Schafernak K, Morgan E, Samet J. Skeletal muscle involvement in B-cell lymphoma: two cases illustrating the contribution of imaging to a clinically unsuspected diagnosis. *Case Rep Radiol.* 2017;2017:2068957.
42. Martins F, Stalder G, Van Der Gucht A, Grandoni F, Cairoli A. Intramuscular follicular lymphoma. *Clin Nucl Med.* 2018;43:682–4.
43. Binici DNR, Karaman A, Timur O, Tasar PNT, Sanibas AV. Primary skeletal muscle lymphoma: a case report. *Mol Clin Oncol.* 2018;8:80–2.

Publisher's Note

Springer Nature remains neutral with regard to jurisdictional claims in published maps and institutional affiliations.

Ready to submit your research? Choose BMC and benefit from:

- fast, convenient online submission
- thorough peer review by experienced researchers in your field
- rapid publication on acceptance
- support for research data, including large and complex data types
- gold Open Access which fosters wider collaboration and increased citations
- maximum visibility for your research: over 100M website views per year

At BMC, research is always in progress.

Learn more biomedcentral.com/submissions

